Wideband dispersion removal and mode separation of Lamb waves based on two-component laser interferometer measurement*

Yan-Feng Xu(徐琰锋) and Wen-Xiang Hu(胡文祥)†

Institute of Acoustics, Tongji University, Shanghai 200092, *China*

(Received 7 April 2017; revised manuscript received 18 May 2017; published online 31 July 2017)

Ultrasonic Lamb waves are considered as a sensitive and effective tool for nondestructive testing and evaluation of plate-like or pipe-like structures. The nature of multimode and dispersion causes the wave packets to spread, and the modes overlap in both time and frequency domains as they propagate through the structures. By using a two-component laser interferometer technique, in combination with a priori knowledge of the dispersion characteristics and wave structure information of Lamb wave modes, a two-component signal processing technique is presented for implementing dispersion removal and mode separation simultaneously for two modes mixture signals of Lamb waves. The proposed algorithm is first processed and verified using synthetic Lamb wave signals. Then, the two-component displacements test experiment is conducted using different aluminum plate samples. Moreover, we confirm the effectiveness and robustness of this method.

Keywords: Lamb wave, dispersion compensation, mode separation, two-component measurement

PACS: 43.35.+d, 43.40.+d **DOI:** 10.1088/1674-1056/26/9/094301

1. Introduction

Lamb waves are widely used in nondestructive testing and evaluation, as well as structural health monitoring, because they can provide more efficient and effective defects inspection methods for plate-like or pipe-like structures compared to those provided by conventional bulk wave inspection techniques.[1–3] Recently, a considerable number of studies pay attention toward corrosion or other defects detection,[4–8] localization,[9,10] and sizing.[11,12] However, because of their nature of dispersion and multimode, for large-range or long-distance testing, Lamb wave signals are frequently becoming considerably complicated owing to the overlapping of multimode wave packets and the duration lengthening as each mode propagates through the structures. Owing to these problems, this type of inspection becomes difficult. On the one hand, dispersion causes the signal energy of guided waves to spread in both space and time when they propagate. This will increase the duration of received signals and decrease the resolution and also the sensitivity owing to the decrease in amplitude. On the other hand, the overlapping of modes makes the signals processing and interpretation complicated and difficult.[13]

The methods of selective excitation for single mode may avoid this problem of dispersion and multimode. These types of method include the comb transducer technique[14] and the angular beam transducer[15] using the narrowband pulse excitation. However, it is difficult to implement, particularly in the high frequency case. Even for the low-frequency case, this narrowband signal may cause a decrease in the resolution when compared with the broadband signal. The other problem is the mode conversion caused by the discontinuities in the propagation path.[16,17] It still makes the received signals multimode and overlapping.

In order to eliminate the dispersion effect of Lamb waves, Alleyne[18] proposed a signal regeneration method, which can obtain a simple waveform at a particular propagation distance by launching a particular dispersive signal. The limitation of this approach is that the input signal should be re-calculated if the propagation distance changes. This causes it to be difficult to use in many cases. There are also some other methods that have been proposed recently, such as a wideband dispersion reversal technique,[19] which try to implement a dispersion self-compensation. The other method presented by Ing and Fink is the time reversal mirror technique to achieve time re-compression of Lamb waves,[20] which automatically focuses the energy of Lamb waves and compensates their dispersion. Wilcox[21] presented another signal processing algorithm for a single dispersive mode. By using a priori knowledge of the dispersion characteristics of this Lamb wave mode, this method can eliminate the effect of dispersion and map signals from time domain to distance domain.

Another problem for NDT of Lamb waves is the mode separation for the multimode overlapping signals. Legg[22] *et al.* attempted to combine dispersion compensation and cross-correlation for enhancing the amplitude of the mode of interest. In general, mode separation is traditionally achieved in the frequency-wavenumber domain using 2D Fourier transform,[23] for which the spatial and temporal data is indispensable. Time-frequency based techniques are typically considered as another effective and popular method for mode separation. Kim[24] employed chirplet transform to de-

*Project supported by the National Natural Science Foundation of China (Grant No. 11374230).

†Corresponding author. E-mail: wxhu@tongji.edu.cn

© 2017 Chinese Physical Society and IOP Publishing Ltd

composition of individual modes from a dispersive and multimodal waveform. Xu *et al.*[25] introduced a mode separation technique based on dispersion compensation.

However, all of these above methods of dispersion removal and mode separation for multimode Lamb waves can only be implemented under certain conditions. It remains a considerably difficult problem particularly for the cases of modes overlapping in both time and frequency domains.

In this paper, we present a novel approach to conduct dispersion removal and mode separation simultaneously for Lamb wave signals of two modes overlapping in both time and frequency domains. In order to implement this signal processing technique, the dual-component displacements, that is, in-plane displacement and out-of-plane displacement signals, are measured by a two-channel laser interferometer.[26] One of the two modes in both in-plane and out-of-plane displacement signals are first mapped from time to distance domains based on its priori theoretical dispersion characteristic to compensate and eliminate its dispersion. Then using two-component displacement signals and the theoretical amplitude ratio of the two modes at the surface of the plate based on the wave structure characteristics of these two modes, the other unwanted mode can be eliminated by using the theoretical relations presented in this paper.

We present the theory and method in Section 2 of this paper, and then we verify the proposed algorithm using theoretical synthetic Lamb wave signals in Section 3. In Section 4, the experiment test is implemented by using a liquid wedge transducer for Lamb waves excitation in an aluminum plate and laser interferometer for signals detection. Moreover, our method is verified by the results of experimental signals processing. Finally, a summary is provided.

2. Theory and methods

2.1. Dispersion compensation method for single Lamb wave mode

Consider a traction-free homogeneous and isotropic plate. A transducer, which is coupled to this plate by some methods (such as liquid wedge), generate a broadband incident pulse $s(t)$. If the material properties are known, the received Lamb wave signals, which can be considered as out-of-displacement, at any propagation distance x can be synthesized by considering the phase shift of each frequency component separately

$$v(x,t) = \int_{-\infty}^{\infty} S(\omega)\, \mathrm{e}^{\mathrm{i}(k(\omega)x-\omega t)}\, \mathrm{d}\omega, \tag{1}$$

where $S(\omega)$ is the frequency spectrum of $s(t)$, and $k(\omega)$ is the wave number of the Lamb wave as a function of frequency ω. The received signal $v(x,t)$ generally spreads continually in space and time owing to the dispersion properties of the Lamb wave.

The above spatial position x can be considered as a new origin $x' = 0$. Subsequently, we can conduct a back-propagation calculation for this received signal $v(x,t)$. When $x' = -x$, the corresponding propagating time will return to the original $t = 0$, and the dispersive signal will be compressed and will be back to be an original simple pulse shape. Using Eq. (1), this calculation can be performed as follows:[21]

$$g\left(x' = -x, t = 0\right) = \int_{-\infty}^{\infty} V(x,\omega)\, \mathrm{e}^{-\mathrm{i}k(\omega)x}\, \mathrm{d}\omega, \tag{2}$$

where $V(x,\omega)$ is the Fourier transform of the received dispersive guided wave signal $v(x,t)$.

For convenience, we rewrite Eq. (2) as

$$g(x) = \int_{-\infty}^{\infty} V(x,\omega)\, \mathrm{e}^{-\mathrm{i}k(\omega)x}\, \mathrm{d}\omega. \tag{3}$$

This calculation achieves a mapping from time to distance for the received signal, and the dispersion is compensated in this procedure. Therefore, $g(x)$ is now a short pulse, or a dispersion-compensated distance-trace. This dispersion compensation method can also be considered to be implemented by multiplying the spectrum of received signal $V(x,\omega)$ by a backward propagation factor $\mathrm{e}^{-\mathrm{i}k(\omega)x}$ in the frequency domain.

The above calculation requires the priori dispersion information of the guide wave under investigation. Theoretical phase velocity dispersion curves for two fundamental modes of Lamb wave in an aluminum plate are depicted in Fig. 1(a). Moreover, their group velocity curves and wave structures (in-plane and out-of-plane displacement distribution, u and v) are presented in Figs. 1(b)–1(d).

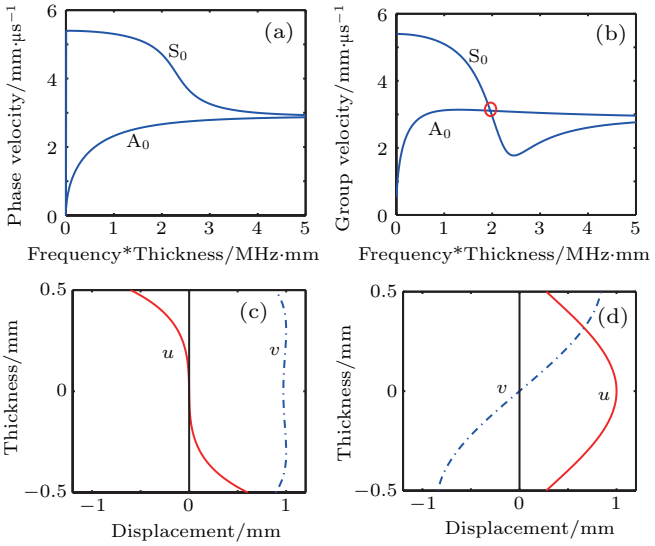


Fig. 1. (color online) Theoretical dispersion curves and wave structures for two fundamental modes of Lamb wave in an aluminum plate. (a) Phase velocity and (b) group velocity curves of S_0 and A_0 modes for an aluminum plate. (c) Wave structure of A_0 for the frequency-thickness product of 2.0 MHz·mm. (d) Wave structure of S_0 with the same frequency-thickness product.

The above dispersion compensation method is only suitable for the single-mode case, and not applicable to the multimode cases. As mentioned earlier, for multimode cases, the other current mode separation and dispersion removal techniques of Lamb waves in time-frequency domain[25] are also infeasible when modes overlap in the time-frequency domain. One case is shown in Fig. 1(b), in which the group velocity curves of two fundamental modes cut across each other. In this case, if the spectrum of measured transient signals covers this frequency area, which is around the crossing point indicated by a red circle, mode separation, and also dispersion removal cannot be achieved effectively.

2.2. Two-component displacements measurement

Compared with conventional piezoelectric transducer-based techniques, laser-based Lamb wave inspection techniques exhibit their advantage in the ability of noncontact detection. Recently, two-component detection techniques have become practical. In this paper, we use a two-channel laser interferometer technique to measure two displacement component signals, that is, out-of-plane displacement and in-plane displacement.

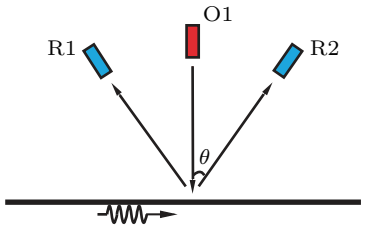


Fig. 2. (color online) Layout of fiber probes of two-channel interferometer for two-component displacement detection. O1 is an optical fiber probe to transmit the incident laser, and R1 and R2 are the fiber probes as receivers to collect the scattered light from the sample surface.

In-plane and out-of-plane displacements at the surface of the sample are measured using a two-channel interferometer. As shown in Fig. 2, an incident laser beam is transmitted from an optical fiber probe O1, which is perpendicular to the surface. Moreover, two other fiber probes R1 and R2 with the same tilted angle θ are applied as receivers for collecting the scattered light from the illuminated surface. The out-of-plane component v can be obtained from a summation of these two signals, and the in-plane displacement u can be acquired from their subtraction[27]

$$\begin{aligned} I_1 + I_2 &\propto \left(\frac{4\pi(1+\cos\theta)}{\lambda}\right) v, \\ I_1 - I_2 &\propto \left(\frac{4\pi\sin\theta}{\lambda}\right) u, \end{aligned} \tag{4}$$

where I_1 and I_2 are, respectively, the light intensity of two receivers with angle θ and light wavelength λ.

2.3. Dispersion compensation and mode separation based on two-component displacement measurement

Consider a common case so that the two fundamental Lamb wave modes A_0 and S_0 exist in the received signal simultaneously, which typically occurs when the frequency-thickness product is not considerably large. According to Eq. (1), the two-component transient displacement signals can be expressed as

$$\begin{aligned} u(x,t) &= \int_{-\infty}^{\infty} S(\omega)\left(A_u(\omega)\,\mathrm{e}^{\mathrm{i}k_1(\omega)x} \right. \\ &\quad \left. + B_u(\omega)\,\mathrm{e}^{\mathrm{i}k_2(\omega)x}\right)\mathrm{e}^{-\mathrm{i}\omega t}\,\mathrm{d}\omega, \end{aligned} \tag{5a}$$

$$\begin{aligned} v(x,t) &= \int_{-\infty}^{\infty} S(\omega)\left(A_v(\omega)\,\mathrm{e}^{\mathrm{i}k_1(\omega)x} \right. \\ &\quad \left. + B_v(\omega)\,\mathrm{e}^{\mathrm{i}k_2(\omega)x}\right)\mathrm{e}^{-\mathrm{i}\omega t}\,\mathrm{d}\omega, \end{aligned} \tag{5b}$$

where $A_u(\omega)$ and $B_u(\omega)$ are, respectively, the amplitude coefficients of the in-plane displacement component for A_0 and S_0 modes. $A_v(\omega)$ and $B_v(\omega)$ are, respectively, the amplitude coefficients of the out-of-plane displacement component for A_0 and S_0 modes. k_1 and k_2 are the wavenumber of modes A_0 and S_0. All coefficients and wavenumbers are functions of frequency.

Now, we assume that S_0 is the mode of interest to be compensated. For our method, the first step is to eliminate the dispersion of this single mode using the algorithm provided in Eq. (3). The spectrums of two-component displacement transient signals $U(x,\omega)$ and $V(x,\omega)$ are multiplied by the backward propagation factor $\mathrm{e}^{-\mathrm{i}k_2(\omega)x}$ of the S_0 mode. Then, the dispersive term of mode S_0 can be compensated, as provided in Eq. (6). However, the dispersive term of another mode A_0 still remains after this performance, because the backward propagation factor of mode S_0 is evidently unable to eliminate the effect of the dispersion of the other mode,

$$\begin{aligned} &U(x,\omega)F(\omega) \\ &= S(\omega)\left(A_u(\omega)\,\mathrm{e}^{\mathrm{i}(k_1(\omega)-k_2(\omega))x} + B_u(\omega)\right), \end{aligned} \tag{6a}$$

$$\begin{aligned} &V(x,\omega)F(\omega) \\ &= S(\omega)\left(A_v(\omega)\,\mathrm{e}^{\mathrm{i}(k_1(\omega)-k_2(\omega))x} + B_v(\omega)\right), \end{aligned} \tag{6b}$$

where $F(\omega) = \mathrm{e}^{-\mathrm{i}k_2(\omega)x}$.

In Eq. (6), the terms $A_u(\omega)\,\mathrm{e}^{\mathrm{i}(k_1(\omega)-k_2(\omega))x}$ and $A_v(\omega)\,\mathrm{e}^{\mathrm{i}(k_1(\omega)-k_2(\omega))x}$, which have different coefficients, but identical phase, can be considered as undesired disturbing terms required to be eliminated. If the in-plane and out-of-plane displacements can be measured, these disturbing terms are possible to be eliminated.

For the two equations in Eq. (6), we use the ratio A_u/A_v to multiply the second equation, and then let them subtract each other; a new expression $L(x,\omega)$, which expresses a pure S_0 mode, can be obtained as

$$L(x,\omega) = \left[U(x,\omega) - (A_u(\omega)/A_v(\omega))V(x,\omega)\right]F(\omega) \tag{7a}$$

$$= \left(B_u(\omega) - \frac{A_u(\omega)}{A_v(\omega)}B_v(\omega)\right)S(\omega). \tag{7b}$$

It is clear that the undesired disturbing terms are eliminated successfully in Eq. (7) with the assistance of two-component

displacements measurement. In Eq. (7a), $U(x,\omega)$ and $V(x,\omega)$ are the spectrums of two-component transient displacement signals, which can be measured and calculated using a two-channels laser interferometer system. From the theoretical wave structure relations of Lamb waves, the coefficients A_u, A_v, B_u, and B_v at the surface of the plate can be calculated. Therefore, the ratio A_u/A_v in Eq. (7a) can be obtained. Calculating Eq. (7a) and performing a Fourier transform for $L(x,\omega)$, and let $t=0$, the distance domain single mode S_0 signal $l(x)$, with its dispersion removal, can be finally obtained as

$$\begin{aligned} l(x) &= \int_{-\infty}^{\infty} L(x,\omega)\,\mathrm{d}\omega \\ &= \int_{-\infty}^{\infty} [U(x,\omega) - (A_u(\omega)/A_v(\omega))V(x,\omega)] \\ &\quad \times \mathrm{e}^{-\mathrm{i}k_2(\omega)x}\,\mathrm{d}\omega. \end{aligned} \tag{8}$$

Using Eqs. (7a) and (8), we can achieve simultaneously the dispersion compensation of one mode and the separation of this mode from the two modes mixture transient signal reliably. The other mode A_0 in this two modes mixture signal can be also separated and dispersion compensated using similar performance.

It is to be noted that the attenuation of guided waves is not considered in the above analysis and calculation. Nevertheless, it is still an effective approach for achieving mode separation and dispersion removal. This can be observed from Eq. (7b) that the mode separation result depends only on the wave structure characteristics of Lamb wave modes and original exciting pulse. The dispersion removal results may be influenced if the attenuation is induced, and it may make the pulse to be restored distortion in some degree when compared to its original pulse shape. However, if the propagation distance is not considerably long and the attenuation is not significant, the result of dispersion compensation will be perfect. The numerical simulation and experimental results in the following two sections will confirm this point.

3. Performance using numerical simulation results

To verify the proposed algorithm in this paper, synthetic Lamb wave signal with two fundamental modes generated in a 1-mm-thick aluminum plate is simulated to conduct this performance. A broadband Gaussian signal as the excitation ultrasonic pulse with a center frequency of 2.0 MHz is considered. At this frequency-thickness product, group velocity curves of A_0 and S_0 modes cross each other as marked in Fig. 1(b), which indicates that the Lamb wave modes may overlap in received signals both in time and frequency domain and it is infeasible for dispersion compensation and mode separation by the current techniques. Figure 3(a) shows two-component synthetic Lamb wave signals for this case,

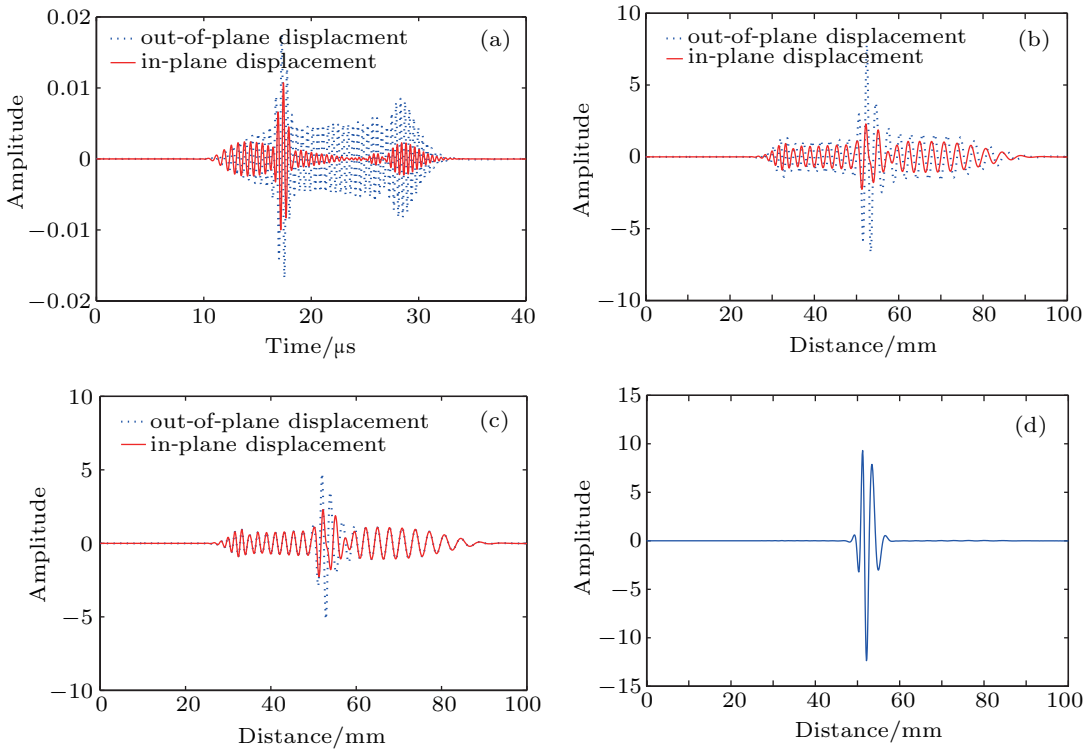


Fig. 3. (color online) (a) Synthetic Lamb wave signals with two modes of A_0 and S_0 excited by an ultrasonic pulse with a center frequency of 2.0 MHz in 1-mm-thickness aluminum plate. (b) Distance-traces mapping after a backward propagation calculation using the propagation function of S_0 mode, i.e., the signals from a Fourier transform of $V(x,\omega)F(\omega)$ and $U(x,\omega)F(\omega)$ on ω. (c) The signals from a Fourier transform of $U(x,\omega)F(\omega)$ and $(A_u/A_v)V(x,\omega)F(\omega)$. (d) Final S_0 distance-trace after mode separation and dispersion removal.

where the propagation distance from the excitation point to the receiving point is 50 mm. For the signals shown in Fig. 3(a), the A_0 mode is a compact wave packet with maximum amplitude because of its nearly constant group velocity around 2 MHz. While the phase and group velocity of the S_0 mode change rapidly at approximately 2 MHz, it makes its duration become considerably lengthy. Its time distribution is from the beginning to the end of the signals. This makes S_0 cross and overlap with the A_0 mode in time, as well as in frequency.

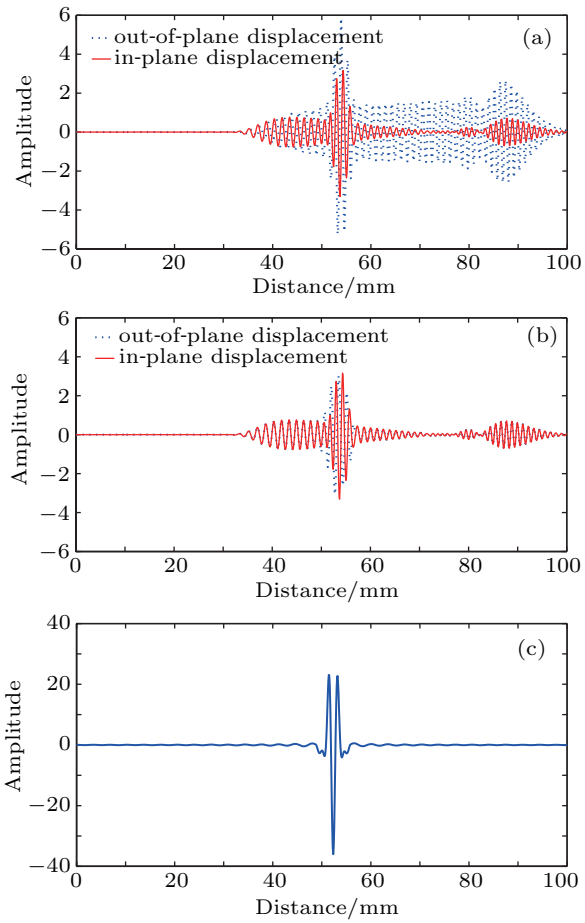


Fig. 4. (color online) (a) Distance-traces mapping after a backward propagation calculation using the propagation function of the A_0 mode for time domain displacement signal. (b) The signals from a Fourier transform of $U(x,\omega)F(\omega)$ and $(B_u/B_v)V(x,\omega)F(\omega)$. (c) Final A_0 distance-trace after mode separation and dispersion removal.

If S_0 is the mode of interest, our target is to use the above algorithm in Eqs. (7a) and (8) to separate it from the mixture signal of two modes and to achieve its time compression or dispersion compensation. Figure 3(b) shows the distance-trace mapping of two-component signals after the performance of a backward propagation algorithm in the frequency domain using the propagation function of S_0 mode $F(\omega) = \mathrm{e}^{-\mathrm{i}k_2(\omega)x}$. Furthermore, using the ratio A_u/A_v, which is the theoretical amplitude ratio of two displacement components for the A_0 mode at the surface of the plate, to calculate $(A_u/A_v)V(x,\omega)F(\omega)$, and then perform a Fourier transform on ω, the out-of-plane signal in the distance domain can be obtained, and it is shown in Fig. 3(c). While the in-plane displacement signal shown in the same figure is identical to that in Fig. 3(b). It can be observed that two signals in Fig. 3(c) coincide completely except the area around the maximum amplitude peak, while these two signals in the same part in Fig. 3(b) exhibit different amplitudes and phases. Figure 3(d) shows the final results, which is a pure S_0 single mode with dispersion removal obtained after a subtraction performance $U(x,\omega)F(\omega) - (A_u/A_v)V(x,\omega)F(\omega)$ was conducted in the frequency domain. Then, a Fourier transform was performed in Eq. (8). It is clear that the propagation distance of this pulse is precisely 50 mm.

It is a similar procedure to separate and compress the A_0 mode from the above mixture signal of two modes. In this case, the propagation function should change to be $F(\omega) = \mathrm{e}^{-\mathrm{i}k_1(\omega)x}$, and the ratio is B_u/B_v. The results are shown in Fig. 4, in which the propagation distance of this pulse is also 50 mm.

There are two criteria to indicate if the modes are compensated and separated accurately. (i) Dispersion is eliminated, and (ii) arrival distance equals the actual propagation distance. Apparently, the processed signal in Figs. 3(d) and 4(c) satisfy these criteria.

4. Experimental results and verification

4.1. Experimental setup

The experimental set-up is shown in Fig. 5. The liquid wedge transducers method[15] was used for generating Lamb waves. A two-channel laser interferometer (Air-1550-TWM, Intelligent Optical System) was used for measuring the two-component displacement signals. An aluminum plate was vertically placed in a water tank, and a part of it was immersed in the water. The incident beam was radiated by an ultrasonic transducer (A314S, 1 MHz/0.75", Panametrics), excited by a pulse signal generator (5077PR, Panametrics) at the central frequency of 1.0 MHz with an angle approximately 24°. Owing to the reason of the beam spreading of the incident wave, both the S_0 and A_0 modes can be excited simultaneously at this angle. About the influence of the transducer's size and incident angle on guided waves excitation, it can also be analyzed theoretically through the normal mode expansion technique.[27] The two-channel signals were measured using the laser interferometer, and acquired using a digital storage oscilloscope (HDO6034, LeCroy) at a sampling rate of 500 MHz and 12 bits A/D conversion accuracy. The measured signals were averaged 100 times and then calculated using Eq. (4) for obtaining the in-plane and out-of-plane signals.

The materials parameters of the aluminum plate used in our experiment are density 2700 kg/m^3, longitudinal wave velocity 6300 m/s, and shear wave velocity 3120 m/s. Two values of plate thickness of 1.5 mm and 2.0 mm were used.

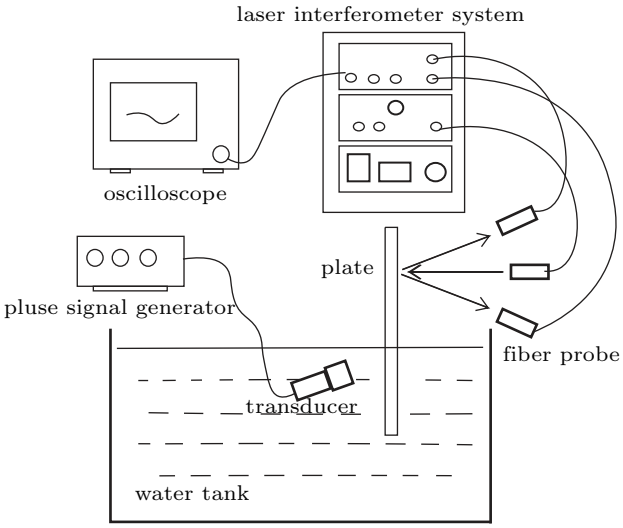


Fig. 5. Schematic of experimental setup.

4.2. Results for 1.5 mm thickness plate

Figure 6(a) shows the Lamb wave signals received from two fiber probes R1 and R2. The in-plane and out-of-plane displacement signals are calculated using Eq. (4), and shown in Fig. 6(b). Figure 7 shows the energy distribution of A_0 and S_0 overlapping with their group velocity spectrum for two plate thickness cases. For the case of 1.5 mm thickness plate, although two modes overlap in the time domain, the majority of the energy distribution of A_0 and S_0 mode are almost not overlapping in the frequency domain, but considerably close around the frequency-thickness product of 2.0 MHz·mm.

By using Lamb waves' dispersion characteristics and the theoretical amplitude ratio of two displacement components, the proposed algorithm was applied to separate and compensate the A_0 and S_0 wave mixture signals shown in Fig. 6(b). Figures 6(c) and 6(d) are the results of this performance for A_0 and S_0 modes, respectively, in which the short pulse signals in the distance domain can be easily used for determining their propagation distance at approximately 80 mm. It should be indicated that the distance between the transducer and aluminum plate was not included in the above propagation distance.

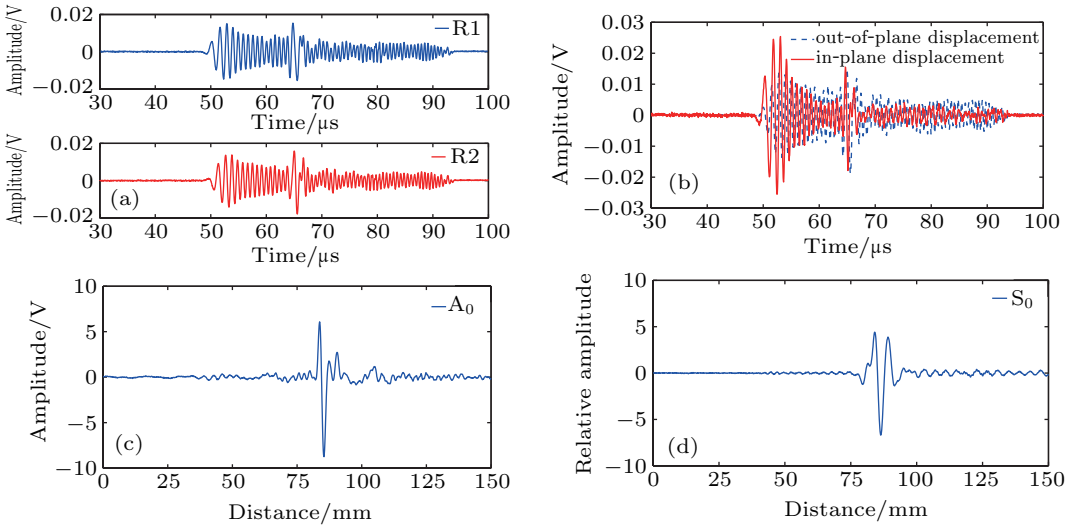


Fig. 6. (color online) (a) Signals received from probe R1 and R2. (b) Two-component displacement signals. (c) A_0 distance-trace after mode separation and dispersion removal. (d) S_0 distance-trace after mode separation and dispersion removal.

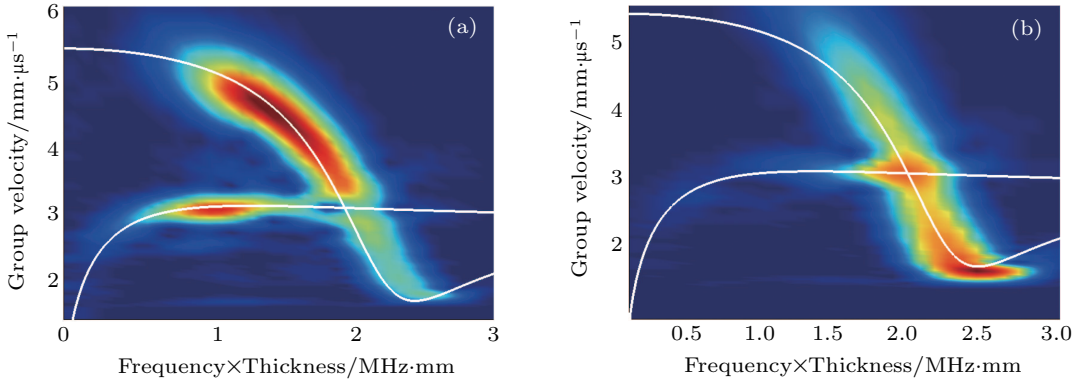


Fig. 7. (color online) Energy distribution of A_0 and S_0 overlapping with their group velocity spectrum for the plate with the thickness of (a) 1.5 mm and (b) 2.0 mm.

4.3. Results for 2 mm thickness plate

Figure 8(a) shows the Lamb wave signals received from two fiber probes R1 and R2 for the case of the 2 mm thickness plate. The calculated results of in-plane and out-of-plane displacement signals are shown in Fig. 8(b). As shown in Figs. 7(b) and 8(b), in this case, A_0 and S_0 are completely overlapping in both time and frequency domains. The duration of the S_0 mode signal is considerably long owing to its notable dispersion in this frequency range. Figures 8(c) and 8(d) are the results of mode separation and dispersion compensation for A_0 and S_0 modes, respectively, for this case, in which the distance-domain short pulse mappings are provided to show a distinct arrival at approximately 100 mm, which is in good agreement with the actual parameter.

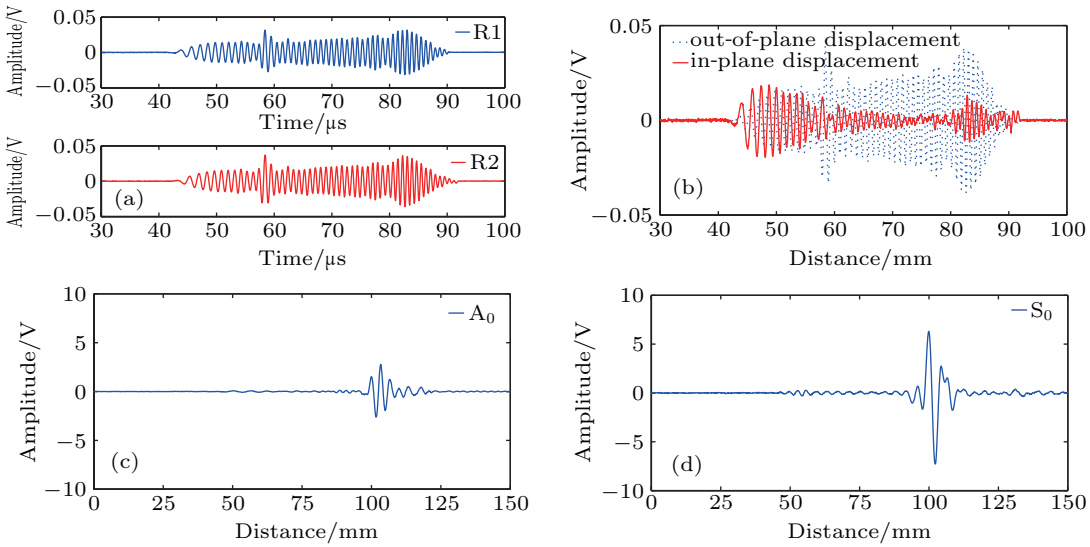


Fig. 8. (color online) (a) Signals received from probe R1 and R2. (b) Two-component displacement signals. (c) A_0 distance-trace after mode separation and dispersion removal. (d) S_0 distance-trace after mode separation and dispersion removal.

5. Conclusion

A novel technique based on two-component displacement (out-of-plane and in-plane displacements) signals measurement was proposed in this paper to compensate and separate two dispersive and overlapping guided wave modes simultaneously, which is infeasible for current and conventional methods, particularly for the case of modes with notable overlapping in both time and frequency domains. In addition to the information of two-component displacement, this technique also requires a priori knowledge of dispersion properties of the two Lamb modes, and their theoretical wave structure information. The principle of this method was presented in this paper. Two-component displacement numerical synthetic signals, which include the two fundamental Lamb modes A_0 and S_0 overlapping in time and frequency domains, excited by an ultrasonic pulse were calculated. Then, the algorithm proposed in this paper was performed for separating and compensating two modes in synthetic signals. Further, this technique was verified by experimental measurement results, in which two aluminum plates with thickness of 1.5 and 2 mm, respectively, were used. Both numerical and experimental results were perfect in the elimination of dispersion effects and separation of the individual mode from the overlapping two modes mixture signals, which demonstrates the validity of this method proposed in this paper. This shows that this technique is useful in guided waves NDE for plate-like or pipe-like structures. We performed further study on defects analysis and localization in plates using this dispersion removal and mode separation technique through both numerical simulation and experimental measurement signals. This will be discussed in other papers.

Acknowledgment

The authors are grateful to Dr. Marvin Klein, Dr. Hengyi Ju, Dr. Hao Wang, and Bin Liu for their help and useful discussions in experimental measurement.

References

[1] Rose J L 2002 *J. Press. Vessel Technol.-Trans. ASME* **124** 273
[2] Rose J L, Pilarski A and Ditri J J 1993 *J. Reinf. Plast. Compos.* **12** 536
[3] Cawley P and Alleyne D 1996 *Ultrasonics* **34** 287
[4] Dixon S, Burrows S E, Dutton B and Fan Y 2011 *Ultrasonics* **51** 7
[5] Benmeddour F, Grondel S, Assaad J and Moulin E 2008 *NDT E Int.* **41** 1
[6] Maslov K and Kundu T 1997 *Ultrasonics* **35** 141
[7] Terrien N, Royer D, Lepoutre F and Deon A 2007 *Ultrasonics* **46** 251
[8] Lee J H and Lee S J 2009 *NDT E Int.* **42** 222
[9] Valle C and Littles J W 2002 *Ultrasonics* **39** 535
[10] Michaels J E and Michaels T E 2007 *Wave Motion* **44** 482
[11] Lu Y, Ye L, Su Z and Yang C 2008 *NDT E Int.* **41** 59
[12] Santos M and Perdigao J 2005 *NDT E Int.* **38** 561

[13] Wilcox P D, Lowe M J S and Cawley P 2001 *NDT E Int.* **34** 1
[14] Li J and Rose J L 2001 *IEEE Trans. Ultrason. Ferroelectr. Freq. Control* **48** 761
[15] Jia X 1997 *J. Acoust. Soc. Am.* **101** 834
[16] Alleyne D N and Cawley P 1992 *IEEE Trans. Ultrason. Ferroelectr. Freq. Control* **39** 381
[17] Morvan B, Wilkie-Chancellier N, Duflo H, Tinel A and Duclos J 2003 *J. Acoust. Soc. Am.* **113** 1417
[18] Alleyne D N, Pialucha T P and Cawley P 1993 *Ultrasonics* **31** 201
[19] Xu K, Ta D, Hu B, Laugier P and Wang W 2014 *IEEE Trans. Ultrason. Ferroelectr. Freq. Control* **61** 997
[20] Ing R K and Fink M 1998 *Ultrasonics* **36** 179
[21] Wilcox P D 2003 *IEEE Trans. Ultrason. Ferroelectr. Freq. Control* **50** 419
[22] Legg M, Yücel M K, Kappatos V, Selcuk C and Gan T 2015 *Ultrasonics* **62** 35
[23] Tian Z and Yu L 2004 *J. Intell. Mater. Syst. Struct.* **25** 1107
[24] Kim C Y and Park K J 2015 *NDT E Int.* **74** 15
[25] Xu K, Ta D, Moilanen P and Wang W 2012 *J. Acoust. Soc. Am.* **131** 2714
[26] Cand A, Monchalin J P and Jia X 1994 *Appl. Phys. Lett.* **64** 414
[27] Rose J L 2004 *Ultrasonic Waves in Solid Media* (Cambridge) p. 200